Elongation of centriolar microtubule triplets contributes to the formation of the mitotic spindle in γ-tubulin-depleted cells

Brigitte Raynaud-Messina*, Laurent Mazzolini, André Moisand, Anne-Marie Cirinesi and Michel Wright

ISTMT, Centre de Recherche en Pharmacologie-Santé, UMR 2587 CNRS-P. Fabre, 3 rue des Satellites, 31 400 Toulouse, France
*Author for correspondence (e-mail: brigitte.raynaud-messina@istmt.cnrs.fr)

Summary

The assembly of the mitotic spindle after depletion of the major γ-tubulin isotype by RNA-mediated interference was assessed in the *Drosophila* S2 cell line. Depletion of γ-tubulin had no significant effect on the cytoskeletal microtubules during interphase. However, it promoted an increase in the mitotic index, resulting mainly in monopolar and, to a lesser extent, asymmetrical bipolar prometaphases lacking astral microtubules. This mitotic accumulation coincided with the activation of the mitotic checkpoint. Immunostaining with an anti-Asp antibody revealed that the spindle poles, which were always devoid of γ-tubulin, were unfocused and organized into sub-spindles. Despite the marked depletion of γ-tubulin, the pericentriolar proteins CP190 and centrosomin were recruited to the spindle pole(s), where they formed three or four dots, suggesting the presence of several centrioles. Electron microscopic reconstructions demonstrated that most of the monopolar spindles exhibited three or four centrioles, indicating centriole duplication with a failure in the separation process. Most of the centrioles were shortened, suggesting a role for γ-tubulin in centriole morphogenesis. Moreover, in contrast to metaphases observed in control cells, in which the spindle microtubules radiated from the pericentriolar material, in γ-tubulin-depleted cells, microtubule assembly still occurred at the poles but involved the elongation of centriolar microtubule triplets. Our results demonstrate that, after depletion of γ-tubulin, the pericentriolar material is unable to promote efficient microtubule nucleation. They point to an alternative mechanism of centrosomal microtubule assembly that contributes to the formation of abnormal, albeit partially functional, mitotic spindles.

Key-words: γ-Tubulin, Centriole, Mitosis, Microtubule assembly

Introduction

In animal cells, the centrosome (composed of the two centrioles and the pericentriolar material) organizes the interphase microtubule cytoskeleton. Following their duplication, the two centriole pairs separate at the onset of mitosis and promote the organization of a bipolar spindle (Wheatley, 1982). Electron microscopic observations and renucleation experiments have shown that the pericentriolar matrix is involved in the nucleation and organization of most of the spindle microtubules (Moritz et al., 1995b; Moritz et al., 1998). Many lines of evidence have suggested a role for γ-tubulin in these processes. In vitro experiments involving pure γ-tubulin or purified γ-tubulin complexes have shown that γ-tubulin plays a role in microtubule assembly (Gunawardane et al., 2000; Leguy et al., 2000; Oegema et al., 1999; Shu and Joshi, 1995; Wiese and Zheng, 2000; Zheng et al., 1995). Microinjection of γ-tubulin antibodies into animal cells disrupts the dynamics of the mitotic spindle and prevents reassembly of the interphase microtubule cytoskeleton (Joshi et al., 1992). In animal cells, cytosolic γ-tubulin is present mainly in two protein complexes. These consist of the small γ-tubulin complex (γ-TuSC), composed of two molecules of γ-tubulin and two associated proteins, and a larger complex [γ-tubulin ring complex (γ-TuRC)], formed by the association of

the γ-TuSCs with at least four other proteins. Current models propose that γ-tubulin is recruited to the centrosome as γ-TuRCs, which are then activated in order to direct the assembly of spindle microtubules (Fava et al., 1999; Félix et al., 1994; Gunawardane et al., 2000; Martin et al., 1998; Murphy et al., 2001; Murphy et al., 1998; Oegema et al., 1999; Stearns and Kirschner, 1994; Tassin et al., 1998; Zhang et al., 2000). Consistent with a role for the γ-tubulin complexes in microtubule nucleation, γ-tubulin is localized to the pericentriolar matrix at the minus ends of the microtubules (Moritz et al., 1995a; Moritz et al., 1995b; Wiese and Zheng, 2000). γ-Tubulin is also present in the centrioles (Fuller et al., 1995; Moudjou et al., 1996) and in the basal bodies (Klotz et al., 2003). In the basal bodies, it is localized within the proximal end of the barrel lumen formed by the nine symmetrical microtubule triplets that elongate from their distal ends to form the nine-axoneme peripheral microtubule doublets of the flagellum (Wheatley, 1982). Consistent with this centriolar localization, silencing of γ-tubulin genes prevented the duplication of the basal-body rows in *Paramecium* (Ruiz et al., 1999), and γ-tubulin was thus assumed to be involved in basal-body morphogenesis by nucleating microtubule triplets (Ruiz et al., 1999).

Despite these findings, several observations are puzzling

regarding the in vivo function of γ-tubulin in microtubule nucleation. In both fungal and animal cells, attempts to deplete γ-tubulin by gene knockouts have not allowed the complete disappearance of the interphase and mitotic microtubules. In *Caenorabditis elegans* embryos depleted of γ-tubulin by either RNA-mediated interference (RNAi) or mutation, the centrosomal asters failed to form during interphase but assembled as cells entered into mitosis, giving rise to collapsed spindles (Strome et al., 2001; Hannak et al., 2002). In other cases, such as *Drosophila* 23C γ-tubulin mutants or *Saccharomyces* γ-tubulin conditional mutants, the spindle microtubules assembled but exhibited low microtubule numbers and/or abnormal structures (Sunkel et al., 1995; Marshall et al., 1996; Spang et al., 1996). These microtubule assemblies could result either from the presence of residual amounts of γ-tubulin or from alternative cryptic microtubule assembly mechanisms that are unfavourable under normal conditions. Microtubule assembly via a chromosome-dependent pathway could account for these observations (for review, see Wittmann et al., 2001). However, no centrosomal mechanism independent of the pericentriolar matrix has yet been demonstrated.

In cultured *Drosophila* cells, two γ-tubulin isotypes are co-expressed, 23C and 37CD (Rubin et al., 2000; Sunkel et al., 1995; Tavosanis et al., 1997; Raynaud-Messina et al., 2001). These isoforms are 83% identical and differ mainly in their C-terminal regions (Rubin et al., 2000; Sunkel et al., 1995; Tavosanis et al., 1997). The 37CD isoform appears to be present at a low level exclusively in the cytoskeletal fraction. By contrast, the 23C isoform, the major γ-tubulin isotype in these cells, can be detected in the cytosolic fraction as both γ-TuSCs and γ-TuRCs. It is also the only isoform extensively recruited to the mitotic poles, probably accounting for the increase of nucleation activity during mitosis.

In order to investigate the mechanisms involved in spindle microtubule assembly under γ-tubulin-deficient conditions, we depleted *Drosophila* cells of the 23C γ-tubulin isotype by RNAi. We observed an increase in the mitotic index associated with an accumulation of cells exhibiting abnormal prometaphase stages, largely monopolar and asymmetrical bipolar figures. Most of the monopolar figures exhibited two or more short centrioles at their poles, suggesting that γ-tubulin plays an essential role in centriole morphogenesis and separation. Moreover, in contrast to the metaphases observed in control cells, in which the spindle microtubules emanated from the pericentriolar material, in the γ-tubulin-depleted cells electronic microscopy revealed a centrosomal microtubule assembly pathway involving the elongation of centriolar microtubule triplets. These results indicate that this pathway, which is associated with chromosome-dependent microtubule assembly, could account for some of the spindle organization that occurs under γ-tubulin-deficient conditions.

Materials and Methods

RNAi

The RNAi treatments were performed in S2 cells (Schneider, 1972) according to Clemens et al. (Clemens et al., 2000). The 23C-γ-tubulin- and Cdk8-encoding double-strand RNAs (dsRNAs), corresponding to nucleotides 18-722 and 1-706 relative to their start codons, respectively, were used. For the depletion of 37CD γ-tubulin, two specific dsRNAs were used. First, a dsRNA targeting positions 4-834

(a highly conserved region between the two *Drosophila* γ-tubulins) depleted the 23C γ-tubulin but not the 37CD isotype, despite a marked reduction in its mRNA level (data not shown). Second, another dsRNA designed to target a divergent region between the two isotypes was directed against the C-terminus of the 37CD γ-tubulin (positions 1062-1276). It did not affect the level of the corresponding protein even after repeated 7-day treatments over a 30-day period.

Briefly, DNA templates were generated by the polymerase chain reaction (PCR). Both PCR primers contained the T7 RNA polymerase minimal promoter sequence followed by a 21 nucleotide sequence complementary to the cDNA. PCR reactions were performed on linearized plasmid templates corresponding to the cDNA clones LD 40196 (23C γ-tubulin), SD 06894 (37CD γ-tubulin) and PBSCDK8 (cdk8) (Leclerc et al., 1996). Purified PCR products (Qiagen, Chatsworth, CA) were transcribed in vitro with the RiboMAX large-scale RNA production system T7 (Promega, Madison, WI). RNAs were treated with RQ1 DNase (Promega), sequentially extracted with phenol-chloroform and chloroform, ethanol precipitated, resuspended in diethyl pyrocarbonate (DEPC)-treated water, and then annealed. In all experiments, the depletion efficiency was checked by immunoblotting for γ-tubulin and the expression of the 37CD-γ-tubulin-encoding mRNA was assessed by reverse-transcription PCR (RT-PCR).

Western-blot analysis

Cell protein extracts were prepared and subjected to western-blot analysis as previously described (Raynaud-Messina et al., 2001). The mouse monoclonal antibody GTU-88 was raised against the amino acid region encompassing residues 38-53 of human γ-tubulin (Sigma-Aldrich, Saint Quentin Fallavier, France). The rabbit polyclonal antibody R70 was raised against the conserved region spanning residues 323-338 of *Aspergillus* γ-tubulin (Julian et al., 1993) and then affinity purified on recombinant human γ-tubulin. The mouse monoclonal antibody 1501 reacted against actin (Chemicon International, Temecula, CA). An Alpha Imager 1200 (Alpha Innotech, San Leandro, CA) was used for the quantifications.

Immunofluorescence staining

The mouse monoclonal antibody T-5168 (Sigma-Aldrich) was used to stain for α-tubulin. The rabbit antibodies R62 and R46 were used for the detection of the 13 C-terminal amino acids of 23C γ-tubulin and the pre-C-terminal amino acid sequence of 37CD γ-tubulin, respectively (Raynaud-Messina et al., 2001). Antibody Rb188 was used to detect CP190 (Whitfield et al., 1988). The rabbit antibody Rb3133, directed against Asp, was a gift from D. M. Glover (University of Cambridge, UK) (Saunders et al., 1997), the rabbit antibody Rb666 (against Bub1) was obtained from C. E. Sunkel (Bausbaa, Lopes and Sunkel, Universitade do Porto, Portugal; unpublished), the rabbit polyclonal antibody R19 (against centrosomin) was from T. C. Kaufman (Howard Hughes Medical Institute, Indiana University, Bloomington, Indiana, USA) and the rabbit antibody against Cid (for identification of the centromere) was from S. Henikoff (Howard Hughes Medical Institute, Fred Hutchinson Cancer Research Center, Seattle, WA) (Henikoff et al., 2000). The cytoskeletal microtubules were observed in cells permeabilized for 1 minute in PEM (100 mM PIPES, 1 mM EGTA, 2 mM MgCl$_2$, pH 6.8) containing 0.5%v/v Triton X-100 and then fixed for 1 hour in PEM containing 1% dimethyl sulfoxide and 3.7%v/v paraformaldehyde, and immunolabelled with the monoclonal antibody T-5168 against α-tubulin. For double immunolabelling, cells were fixed for 20 minutes in DES culture medium (Invitrogen, Cergy Pontoise, France) containing 3.7% v/v paraformaldehyde, permeabilized for 2 minutes in methanol (–20°C) and then incubated with the appropriate antibodies. For double labelling of γ-tubulin or Asp with α-tubulin, antibodies against Asp or γ-tubulin were added to the cells, which

were incubated for 1 hour at 37°C before the antibodies against α-tubulin were added and the cells were incubated for another 1 hour at 37°C, followed by overnight at 4°C. Alternatively, for double labelling of α-tubulin and CP190 (or centrosomin), the antibodies against α-tubulin and CP190 (or centrosomin) were added sequentially to the cells, which then were processed with fluorescein isothiocyante (FITC) and tetramethylrhodamine isothiocyanate (TRITC)-conjugated secondary antibodies (Santa Cruz Biotechnology, Santa Cruz, CA).

For the renucleation experiments, cells were incubated at 4°C for 2 hours and then allowed to recover by incubating in DES medium at 22°C. After 2 minutes, the cells were rapidly fixed in cold methanol (–20°C, 30 minutes) and double stained with the antibodies against α-tubulin and centrosomin.

Electron microscopy

Cells were fixed by successive addition of 0.25 volumes of PHEM (60 mM PIPES, 25 mM HEPES, 10 mM EGTA, 2 mM MgCl$_2$, pH 7.0) containing 2.5% glutaraldehyde to 1 volume of culture medium at 0 hours, 3 hours, 6 hours and 9 hours after commencing the procedure. Cells were recovered at 12 hours and processed for electron microscopy. Tannic-acid counterstaining was performed to determine the number of protofilaments (Tilney et al., 1973).

Results

RNAi strongly reduced the level of 23C γ-tubulin in cultured *Drosophila* cells

The levels of 23C and 37CD γ-tubulins were characterized in S2 cell extracts by labelling with the two anti-γ-tubulin antibodies GTU (two exposures were performed) and R70 (Fig. 1A, see controls, lane c). As revealed by these antibodies, 23C γ-tubulin was the major isotype expressed in S2 cells. RNAi directed against 23C γ-tubulin strongly downregulated its expression (Fig. 1A, lanes γ23C). This treatment altered neither the low level of expression of 37CD γ-tubulin (Fig. 1A, second and third panels) nor the level of actin (Fig. 1A, fourth panel) used as a negative control. We reproducibly observed a reduction of at least 90-95% in the 23C γ-tubulin levels (Fig. 1B). This inhibitory effect was stable for at least 9 days. A partial reversal of inhibition was observed at day 14 after treatment (Fig. 1C, lane R14). To control for the specificity of RNAi, cells were subjected to RNAi directed against Cdk8, a transcription factor unrelated to the microtubule cytoskeleton (Barette et al., 2000; Leclerc et al., 1996). Depletion of Cdk8 did not affect the levels of γ-tubulin and actin (Fig. 1D).

### Depletion of 23C γ-tubulin led to a mitotic accumulation

Downregulation of 23C γ-tubulin did not seem significantly to affect the interphase microtubule cytoskeleton. However, whatever the schedule of treatment, the mitotic indices were significantly higher in 23C-γ-tubulin-depleted cells than in control cells (Table 1). When a single RNAi treatment was given on day 1, we noticed a decrease of the mitotic indices for both the control and the treated cells 7 days after

treatment. To check whether this reduction in the mitotic index was related to exhaustion of the medium, we applied two successive RNAi treatments (days 1 and 5), which allowed a refeeding on day 5. The mitotic indices observed on day 7 were significantly increased (Table 1). Using this protocol, we reproducibly observed mitotic indices of 1.5-2.0% in control cells versus 9-13% in treated cells (five independent experiments).

Depletion of 23C γ-tubulin induced abnormal mitotic figures

In order to determine whether the increase in mitotic index was accompanied by an accumulation of cells at a specific stage of mitosis, we characterized the microtubule cytoskeleton by immunofluorescence. We observed mitotic figures without a
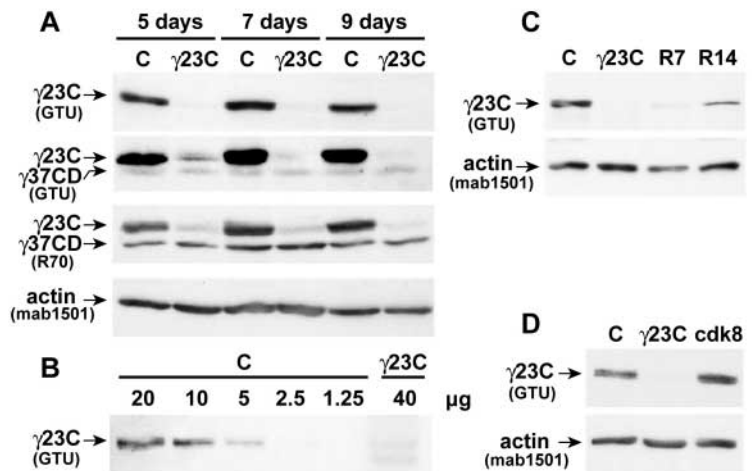
Fig. 1. Specific depletion of 23C γ-tubulin by RNA-mediated interference (RNAi). (A) Depletion kinetics. Control cells (C) and cells subjected to 23C γ-tubulin RNAi treatment (γ23C) were harvested after 5 days, 7 days and 9 days of culture. Total-protein extracts (50 µg) were analysed by immunoblotting. From day 5 to day 9, a strong and specific depletion of 23C γ-tubulin was observed. (First and second rows) Monoclonal GTU γ-tubulin antibody staining. The 37CD γ-tubulin band was not visible when the signal from 23C γ-tubulin was not overexposed (first row) and could be visualized only by reacting blots with more antibody and then overexposing the membranes (second row). (Third row) Purified polyclonal R70 antibody staining. Here, 37CD γ-tubulin also appeared to be less abundant than the 23C γ-tubulin. (Fourth row) The monoclonal antibody mab1501 was used to detect actin as an internal loading control. (B) Quantification of the depletion of γ-tubulin. The γ-tubulin content of 40 µg of an extract from cells submitted to a 7-day RNAi (γ23C) was compared by immunoblotting with that of serial loadings (20-1.25 µg) of protein extracts from control cells (C) and quantified by densitometry analysis. 23C γ-tubulin RNAi reduced the γ-tubulin level by at least 95%. (C) Reversibility of γ-tubulin depletion. Extracts (50 µg), prepared from control cells (C), 7-day-treated cells (γ23C) or from cells that had been treated with the γ23C RNA for 7 days, then washed and maintained in culture for a further 7 days (R7) and 14 days (R14) without RNAi were analysed by immunoblotting with the GTU (against 23C γ-tubulin) and mab1501 (against actin) antibodies. The 23C γ-tubulin signal reappeared 14 days after the removal of the γ23C RNA by washing. (D) Depletion specificity. Extracts (50 µg) from cells submitted to a 7-day RNAi treatment against either 23C γ-tubulin (γ23C) or the transcriptional factor Cdk8 (cdk8) were immunoblotted with the antibodies GTU (against 23C γ-tubulin) and mab1501 (against actin). Depletion of Cdk8 did not affect the levels of 23C γ-tubulin and actin.

Table 1. Mitotic accumulation after 23C-γ-tubulin depletion

		Mitotic index (%)	
Treatment	Incubation time (days)	Control	Tγ23C
Day 1	5	2.3% (2.0-2.6%) *n*=10,233	6.5% (6.0-7.0%) *n*=10,690
	7	0.9% (0.8-1.0%) *n*=10,022	4.1% (3.7-4.5%) *n*=10,429
	9	0.15% (0.1-0.2%) *n*=10,015	0.35% (0.2-0.5%) *n*=10,035
Days 1 and 5	7	2.0% (1.7-2.3%) *n*=10,206	13% (11.6-14.4%) *n*=2,300

The mitotic indices (M.I.) [i.e. the proportion of cells undergoing mitosis divided by total cell number (*n*)] were determined after chromosome staining (with DAPI) and immunolabelling of the microtubule cytoskeleton (with antibodies against α-tubulin). These quantifications were performed in control cells and in cells treated by RNAi against 23C γ-tubulin either once (day 1; M.I. quantifications after 5 days, 7 days and 9 days) or twice (days 1 and 5; M.I. quantification after 7 days). All confidence intervals (in parentheses) were calculated for a probability of 95%. Data from a representative experiment are presented. Four additional experiments giving comparable results were performed.

distinct microtubule polarity, monopolar prometaphases, bipolar prometaphases, elongated mitoses and rare post-metaphase stages (Table 2). In all cases, the mitotic figures were devoid of 23C γ-tubulin signal (Table 3, Fig. 2B-C,F-G, Fig. 3B-E), whereas, in control prometaphase/metaphases, 23C γ-tubulin signal was present at the two poles and in the spindle (98%, *n*=116, 95% C.I.=96-100; Fig. 2A,A′). Under our experimental conditions, the polar localization of 37CD γ-tubulin was maintained after 23C γ-tubulin RNAi. In monopolar figures, only the spot corresponding to microtubule focalization was stained, whereas, in bipolar spindles either a single pole or both poles were labelled (Fig. 2L,M). Surprisingly, after 23C γ-tubulin depletion, all mitotic figures lacked astral microtubules (Figs 2, 4).

Non-polar figures

Typical prophases accounted for about 6% of the mitotic stages observed in control cells. These were mostly absent after 23C γ-tubulin depletion. By contrast, we observed figures with no evident microtubule polarity (13%), which corresponded either to late prophase stages or to a highly unstructured spindle (Table 2).

Monopolar spindles

The most common mitotic figures observed after 23C γ-tubulin depletion were monopolar spindles (Table 2, 60%). Some 10-22% of the γ-tubulin-depleted monopolar figures consisted of an aster of microtubules radiating from a central pole towards the chromosomes (Fig. 2C), which formed a rosette or an

Table 2. Cell repartition in the different mitotic stages after 23C-γ-tubulin depletion

Mitotic stages	Control	Tγ23C
Prophases	6% (4-8%)	0% (0-1%)
No polarity	0% (0-4%)	13% (10-17%)
Monopolar spindles	0% (0-4%)	60% (57-63%)
Bipolar spindles	36% (29-43%)	13% (10-17%)
Elongated spindles	0% (0-4%)	12% (9-15%)
Late mitotic stages	58% (53-63%)	2% (1-3%)

The mitotic stages were determined after chromosome staining (with DAPI) and immunolabelling of the microtubule cytoskeleton (with antibodies against α-tubulin) in control cells (*n*=102) and in 7-day 23C-γ-tubulin-treated cells (*n*=429). All confidence intervals (in parentheses) were calculated for a probability of 95%. Data from a representative experiment are presented. Four additional experiments giving comparable results were performed.

indistinct mass. The remaining 78-90% constituted a single microtubule conical half-spindle (Fig. 2B,D,E). Both of these monopolar figures corresponded to a prometaphase stage as demonstrated by the presence of fully condensed chromosomes that were either organized as a curved plate or scattered on the spindle (Fig. 2B-E). The chromatids were unseparated, as revealed by Cid staining (data not shown) and the mitotic checkpoint was activated, as evidenced by kinetochore staining with antibodies against Bub1 (Fig. 2D,E) (Basu et al., 1999).

Bipolar spindles

Another consequence of RNAi was a decrease in the frequency of bipolar mitoses (Table 2, 13% versus 36% in control). These bipolar figures were composed of multiple small spindles leading to large poorly focused or unfocused poles (Fig. 2F-I). They corresponded to prometaphase stages as demonstrated by the presence of condensed unseparated chromatids (Cid staining, data not shown), which were often misaligned (Fig. 2H) or partially dispersed over the spindles, and by a strong Bub1 signal at the kinetochores (Fig. 2H,I).

Elongated spindles

Atypical elongated spindles, which were rarely observed in control cells, were significantly increased in cells after γ23C-tubulin depletion (Table 2, 12%). The kinetochores were always stained by Bub1 antibodies, suggesting that the cells failed to enter metaphase (Fig. 2J-K). The chromosomes were either scattered (Fig. 2J) or tended to accumulate at the two extremities of the spindle (Fig. 2K). Some of these figures could result from either the overall modification of the shape of a bipolar spindle (Fig. 2J) or the elongation of the microtubules of a monopolar spindle (Fig. 2K), as suggested by asymmetrical or symmetrical polar staining (Table 3). In both cases, despite the Bub1 kinetochore labelling being indicative of an active mitotic checkpoint, a process similar to anaphase B occurred, even though anaphase A was not fully completed (Cid staining, not shown).

Late mitotic stages

The proportion of cells able to proceed towards the late stages of mitosis was markedly reduced after RNAi (Table 2, 2% versus 58% in control). These figures could be clearly assigned to anaphase, telophase and cytokinesis (Fig. 3), even if individual lagging chromosomes (Cid staining, data not

Table 3. Spindle-pole labelling after 23C-γ-tubulin depletion

| Staining | Prometaphases | | Atypical elongated spindles |
	Monopolar	Bipolar	
γ-Tubulin	1.7% (0-3.6%) *n*=177	6.6% at one pole (3-10%) *n*=197	0% (0-0.3%) *n*=20
Asp	100% (94-100%) *n*=66	6.0% at one pole (2-13%) *n*=85 94% at both poles (87-98%) *n*=85	19% at one pole (5-51%) *n*=16 81% at both poles (48-95%) *n*=16
CP190	97% (94-100%) *n*=102	51% at one pole (29-61%) *n*=35 49% at both poles (21-59%) *n*=35	88% at one pole (48-100%) *n*=16 12% at both poles (2-44%) *n*=16
Centrosomin	100% (90-100%) *n*=415	27% at one pole (19-34%) *n*=98 73% at both poles (65-81%) *n*=98	55% at one pole (25-57%) *n*=20 44% at both poles (43-75%) *n*=20

Cells were treated twice with RNAi against 23C-γ-tubulin and observed at day 7. The spindles were labelled with antibodies against α-tubulin, whereas the poles were challenged with antibodies against γ-tubulin, Asp, CP190 or centrosomin. All confidence intervals (in parentheses) were calculated for a probability of 95%.

shown) and/or unequal chromosome distribution were sometimes observed. These lagging chromosomes were devoid of Bub1 staining (not shown). During cytokinesis, the characteristic microtubule bundles were present despite the absence of γ-tubulin labelling (Fig. 3D,E), and control cells exhibited a strong centrosome and mid-body γ-tubulin staining (Fig. 3A,A′). In most cases, cytokinesis was apparently bipolar, suggesting that it proceeded from bipolar figures (Fig. 3B-D). Monopolar cells undergoing cytokinesis were rarely observed (Fig. 3E), in contrast to γ-tubulin-depleted *Drosophila* spermatocytes, which possess a less efficient mitotic checkpoint (Sampaio et al., 2001). The presence of these abnormal post-metaphase stages is consistent with several lines of evidence that point to a role for γ-tubulin in mid-body formation in mammalian cells (Julian et al., 1993; Shu et al., 1995). This observation was supported by phenotypic analysis after recovery from RNAi, which revealed, first, a decrease in the number of monopolar prometaphases to 9% (*n*=164; 95% C.I.=5-14) and an increase in the post-metaphase stages to 49% (95% C.I.=41-57), and, second, many prometaphase figures that exhibited chromosome numbers higher than 2N (53%, *n*=58; 95% C.I.=37-63) or multiple poles (10%, 95% C.I.=4-20).

The ratio of prometaphase figures to anaphases/telophase figures, which ranged from 0.2 to 0.65 in control cells, was increased to between 7 and 46 in treated cells, depending on the experiment (*n*=5) (Table 2). Therefore, we conclude that the 6-fold to 6.5-fold increase in the mitotic index (Table 1) resulted both from the higher frequency of unpolarized, monopolar and unfocused bipolar prometaphases, concomitant with a marked decrease in the proportion of cells exiting from mitosis.

Spindle abnormalities in γ-tubulin-depleted cells are associated with polar defects

The absence of a 23C γ-tubulin signal at the spindle poles suggested that the formation of monopolar and bipolar spindles was not directly under the control of the major cellular γ-tubulin (Table 3; Fig. 2). However, many lines of evidence based on independent approaches suggested that at least some spindle microtubules nucleated from the centrosomes towards the chromosomes. First, as revealed by immunofluorescence and electron microscopy, there were, in addition to the microtubules that interacted with the kinetochores, others

that extended away from chromosomes (Fig. 4A, Fig. 5A). Second, in γ-tubulin-depleted cells, the proteins CP190 and centrosomin retained their polar localization (Fig. 4A). Third, renucleation proceeded in RNAi-treated mitotic figures from one or two focalization points (Fig. 4B).

In the prometaphase figures of the control cells, Asp (Saunders et al., 1997), a protein that accumulates at the minus ends of the spindle microtubules (Riparbelli et al., 2002; Wakefield et al., 2001), was localized to the face of the centrosomes that made contact with the spindle microtubules. In the treated cells, Asp was usually clustered around the poles in both mono- and bipolar prometaphase figures, but formed punctate dots (Table 3, Fig. 4Aa-b,g-h). This staining pattern showed that the microtubules retained their normal orientation but were organized as several distinct arrays assembled from the polar regions. This was confirmed using immunostaining for CP190 (Fig. 4Ac-d,i-j) and centrosomin (Fig. 4Ae-f,k-l) as markers of the pericentriolar material. CP190 relocalizes to the pericentriolar material during mitosis (Whitfield et al., 1988) and is absent from the poles of acentriolar metaphase cells (Debec et al., 1995). A CP190 signal was detected at the pole in nearly all the monopolar figures (Table 3; Fig. 4Ac-d). A variable number of CP190 dots was observed, with a maximum of four dots (Fig. 4Ad). In the bipolar figures, about one-half of the spindles showed CP190 signals at both poles (Fig. 4Ai), whereas, in the other half, CP190 dots were observed in one spindle pole only (Table 3, Fig. 4Aj). Centrosomin is an essential component for centrosome assembly and function (Li and Kaufman, 1996; Megraw et al., 1999). It associates with the pericentriolar matrix during mitosis and is dispersed at interphase (Megraw et al., 2001). As for CP190, centrosomin was recruited as variable number of dots localized to the pole in nearly all monopolar figures (Table 3, Fig. 4Ae-f), whereas, in bipolar prometaphases, it was present at one pole or both poles (Table 3, Fig. 4Ak-l). Because CP190 and centrosomin were recruited to the polar structures, this indicated that mitotic centrosomal maturation had occurred to some extent, even in the absence of a detectable amount of 23C γ-tubulin. To determine whether these centrosomin-stained structures were functional, cold disassembly/reassembly experiments were performed. In control cells, renucleation always occurred from two opposed centrosomin-stained spots, giving rise to a bipolar structure (not shown). In RNAi-treated cells, renucleation proceeded from one or two focalization points (Fig. 4B) distinct from the chromosomes. In all cases, these microtubule-

organizing centres were decorated by the centrosomin antibody. The morphology of the renucleated microtubule bundles indicated that they could emerge from either initial monopolar or bipolar figures. Hence, it is likely that the mitotic figures generated after RNAi involved polar microtubule assembly, although other nucleation and organization mechanisms that were dependent on the chromosomes and motor proteins could not be excluded. Moreover, the pattern of

CP190 and centrosomin staining suggested that centriole duplication had occurred but that the centrioles had failed to separate in the monopolar and at least some of the bipolar figures.

γ-Tubulin is required for efficient centriole separation and morphogenesis

The hypotheses we raised after observing the presence of multiple CP190 and centrosomin dots at the poles of most spindles were supported by our electron microscopic observations. In most reconstructions (70%; n=27, 95% C.I.=54-88) obtained from serial thin sections, three or four centrioles were observed at the monopolar spindle poles (Fig. 5B1-4), whereas two centrioles were detected at both poles in bipolar metaphases in control cells. Hence, depletion of 23C γ-tubulin did not prevent the triggering of centriole duplication but did impair their separation in the monopolar prometaphases, perhaps owing to modifications in the dynamics of the microtubules involved in this process. Consistent with the presence of the CP190 signal at both poles in half of the bipolar prometaphases, electron-microscopic observations of serial thin sections showed that centriole separation was possible in this case, although it did not always occur (not shown).
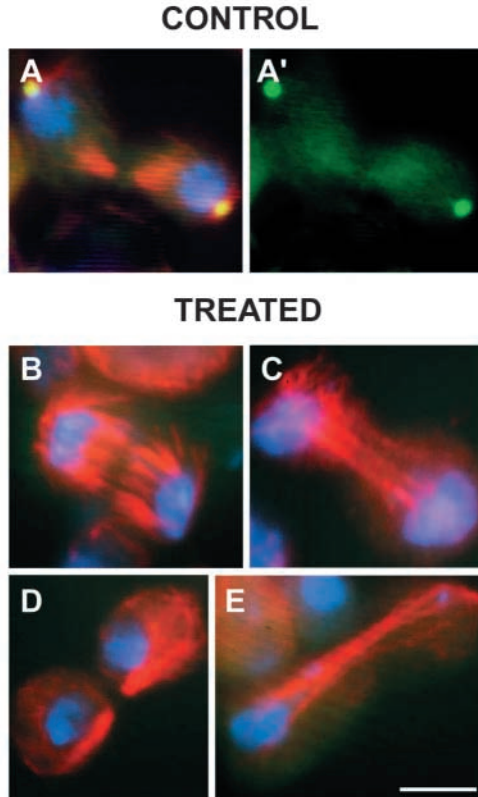
Centrioles exhibit a typical radial structure composed of microtubule triplets or doublets in cross sections, and are unusually short in *Drosophila* cells (Gonzales et al., 1998). After γ-tubulin depletion, the centrioles were of normal width, excluding the possibility that they corresponded to procentrioles but, surprisingly, most of them were markedly shortened (Fig. 6), suggesting that centriole assembly was incomplete.
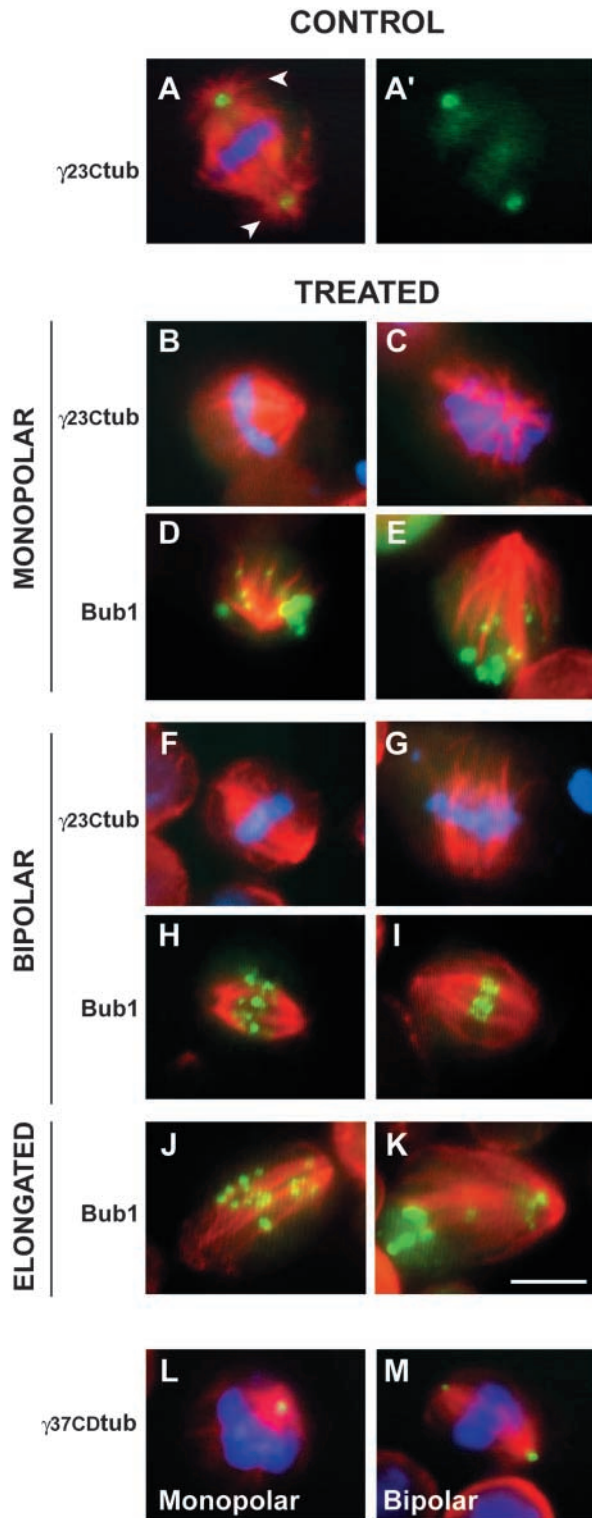
Fig. 2. Prometaphase stages observed after 23C γ-tubulin depletion. Three characteristic mitotic figures were observed after 23C-γ-tubulin depletion: monopolar, bipolar and elongated spindles. Chromosomes were stained with DAPI (blue), microtubules with antibody against α-tubulin (red), whereas 23C-γ-tubulin, Bub1 or 37CD-γ-tubulin immunostaining appeared in green. Scale bar, 5 μm. (A,A′) Control metaphase, showing α-tubulin and 23C γ-tubulin merged staining (A) and γ-tubulin staining only, showing the presence of 23C γ-tubulin at the two poles and in the two half-spindles (A′). All chromosomes were localized to the chromosomal plaque. The two poles exhibited astral microtubules (arrowheads). (B-M) γ-Tubulin-depleted cells. (B-E) Monopolar figures. No γ-tubulin signal could be detected (B,C). Generally the microtubules radiated preferentially from a single region, giving an overall conical shape. The fully condensed chromosomes constituted a plaque (B) or were dispersed in the spindle (C-E). The shape of the single pole was variable (compare B and C) but always devoid of astral microtubules. In all cases, the kinetochores were labelled by Bub1 antibodies (D,E). (F-I) Bipolar figures. The two opposite poles defined by the microtubules were devoid of astral microtubules and of a 23C-γ-tubulin signal (F,G). Although the condensed chromosomes could constitute a typical chromosomal plaque (F,I), more often, some chromosomes were not aligned on the plaque (H) or were even scattered over the spindle. Their kinetochores were always labelled by Bub1 antibodies (H,I). (J,K) Elongated figures. The chromosomes were either scattered (J) or unequally distributed at each pole (K). In all cases, the kinetochores were labelled by Bub1 antibodies. (L,M) 37CD-γ-Tubulin staining, which was present at the pole(s) of formed spindles.

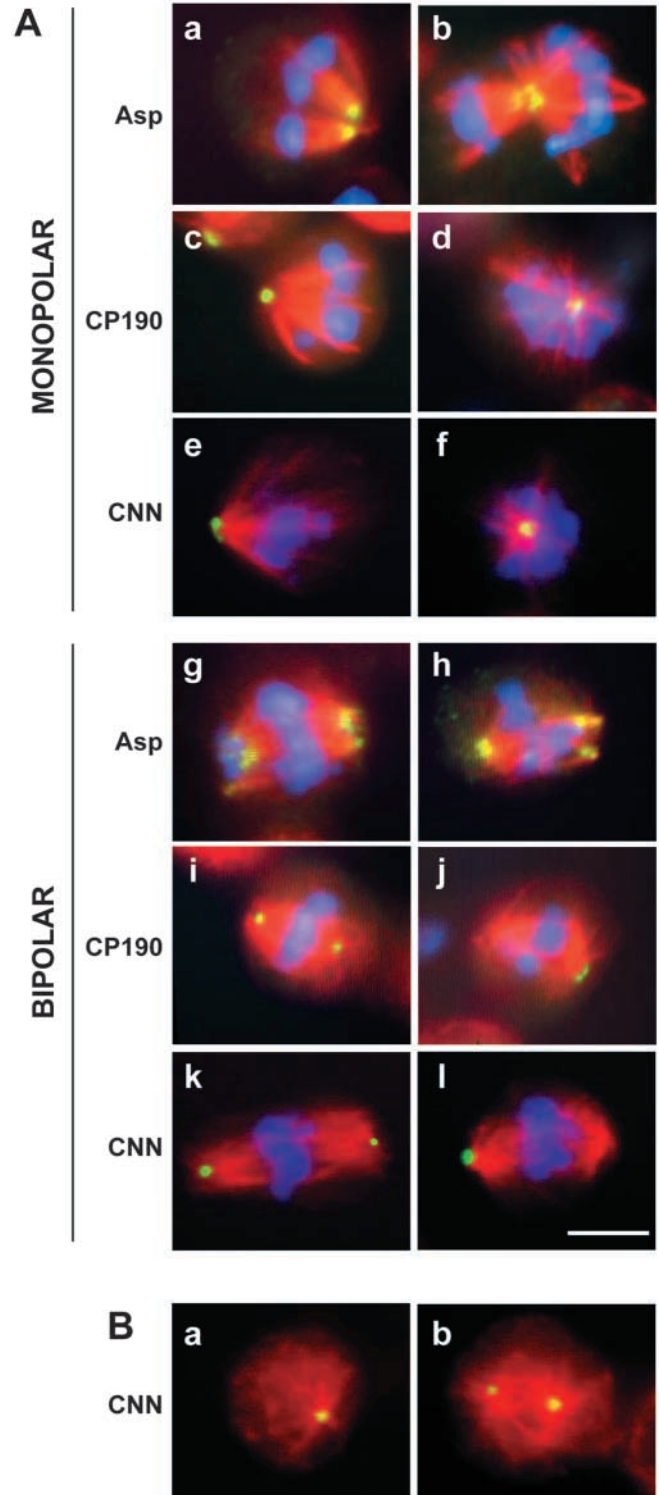## Elongation of centriolar microtubules contributes to spindle formation

In the monopolar metaphases, the mitotic microtubules were organized around a pole characterized by the presence of supernumerary centrioles. However, in contrast to control cells,
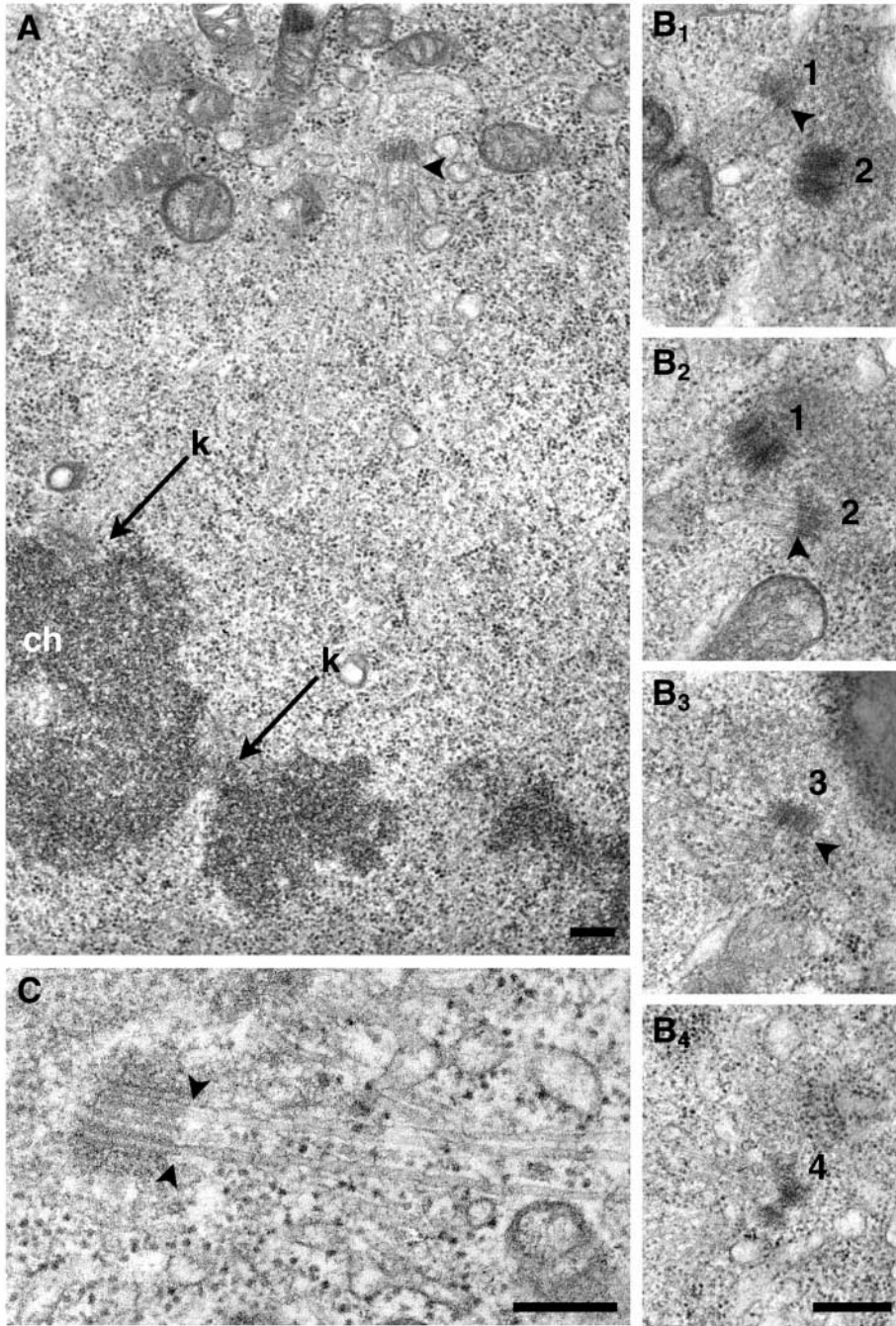
the microtubules did not seem to be nucleated from the pericentriolar material. Electron microscopic observations showed that most of them appeared to be associated with one extremity of the centriole cylinder and in apparent continuity with the centriolar microtubules (Fig. 5A-C, arrowheads). The orientation of the centriolar microtubules in three-dimensional reconstructions showed that the spindle microtubules were assembled from the distal end of the centriole. Most of the

Fig. 3. Post-metaphase figures observed after 23C-γ-tubulin depletion. Chromosomes appear in blue, microtubules in red, and the staining in green corresponds to γ-tubulin. (A,A′) Control cytokinesis showing α-tubulin and γ-tubulin merged staining (A) and γ-tubulin staining only, showing the presence of 23C γ-tubulin at the two poles and in the mid-body (A′). (B-E) Anaphase (B), telophase (C) and cytokinesis (D,E) after γ-tubulin depletion. None of these figures exhibited γ-tubulin signals (absence of green staining). Cytokinesis was generally symmetrical (D) and exceptionally asymmetrical (E). Scale bar, 5 μm.

Fig. 4. Characterization of the poles in monopolar and bipolar figures after 23C-γ-tubulin depletion. (A) Chromosomes appear in blue and microtubules in red, and the staining in green corresponds to the polar mitotic markers Asp (a,b,g,h), CP190 (c,d,i,j) or centrosomin (e,f,k,l). (Aa-f) Monopolar figures. Asp labelling was always exclusively localized to the single pole in several dots corresponding in most cases to sub-spindles (a,b). CP190 labelling was concentrated at the pole as between one and four dots (d). Centrosomin (CNN) was also concentrated at the pole, usually as a large and irregular structure (e,f). (Ag-l) Bipolar figures. Asp was always localized to the two poles, where, in most cases, it constituted a large area composed of two to five dots associated with each sub-spindle (g,h). CP190 and centrosomin labelling were present as one (i) or several (k) dots located at both poles or at one pole (j,l). (B) Renucleation in γ-tubulin-depleted cells. Microtubule arrays (red) renucleated from one or two centrosomin-labelled spots (green) after cold depolymerization. Scale bar, 5 μm.

Fig. 5. Electron microscopic characterization of the poles in monopolar figures after γ-tubulin depletion. (A) Overall image of a monopolar prometaphase. The microtubules from the polar region defined by short centrioles (arrowheads) interacted with the kinetochores (k) of the chromosomes (ch) or passed through the chromosomal mass. (B1-4) Serial thin sections of a pole. The presence of four short centrioles (labelled 1 to 4) shows that, despite depletion of the major cellular γ-tubulin, centriole duplication but not separation took place. (C) Elongation of the centriole microtubules. The spindle microtubules resulted at least partly from the elongation of the distal ends of centriolar microtubules (arrowheads). Scale bars, 0.2 μm.
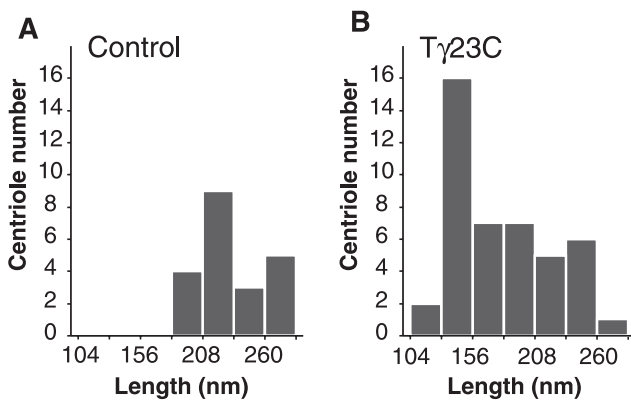
Fig. 6. Centriole length in γ-tubulin-depleted cells. The length of interphase and mitotic centrioles was determined on longitudinal sections obtained by electron microscopy from control (A) and treated (Tγ23C) (B) cells. The two length distribution profiles were significantly different as checked by a homogeneity test based on variance analysis: an experimental score of 41 against a theoretical score of 7 for a security of 99% [according to Snedecor's tables (De Muth, 1999)] indicating that γ-tubulin depletion reduces centriole length.

mitotic microtubules exhibited 13 protofilament structure, with sections revealing 1, 14 and 2 microtubules with 12, 13 and 14 protofilaments, respectively (data not shown). Moreover, this unexpected assembly pathway and the inability of the pericentriolar material to nucleate microtubules could account for the absence of astral microtubules (Figs 2, 4).

Discussion

We have used RNAi to deplete the major γ-tubulin isotype significantly in cultured *Drosophila* S2 cells. Only a few cells escaped this treatment, because less than 0.7% of all mitotic cells presented a bipolar morphology with a positive 23C γ-tubulin signal at both poles. Depletion of 23C γ-tubulin caused S2 cells to accumulate in mitosis, with an active mitotic checkpoint. They exhibited abnormal prometaphase stages, characterized by unseparated condensed chromatids and spindle poles with supernumerary short centrioles. The emergence of a characteristic phenotype (i.e. monopolar prometaphase figures) prompted us to investigate the mechanism of spindle organization in 23C-γ-tubulin-depleted cells. Our investigations revealed that, under γ-tubulin-deficient conditions, the pericentriolar material was unable efficiently to promote microtubule nucleation. Our observations point to the involvement of a previously undescribed centrosomal mechanism of microtubule assembly that operates via elongation of the distal centriolar extremities.

After depletion of 23C γ-tubulin, the duplicated centrioles were present at the one pole of the monopolar prometaphase figures and at only one of the two poles in at least half of the bipolar figures, indicating a segregation failure. This phenomenon has also been suggested to occur in *Drosophila Dgrip91* mutants (Barbosa et al., 2000). Observations made on mammalian cells have demonstrated that the relative positions of the two centriole pairs depend partly on the dynamics of the microtubule cytoskeleton (Jean et al., 1999). Hence, after γ-tubulin depletion, it is likely that the microtubule subnetwork involved in the separation of the centriole pairs underwent modifications in either its dynamics or in its density. Despite the lack of ultrastructural studies excluding morphogenetic and/or separation defects, basal-body duplication has been reported to be impaired after silencing of the γ-tubulin-encoding genes in *Paramecium* (Ruiz et al., 1999). This discrepancy with our observations could result from differences in the timing of centriole and basal-body duplication, and the many rounds of basal-body duplication in *Paramecium* leading to many basal bodies. Thus, it is possible that the critical concentration of γ-tubulin required for centriole duplication is lower than the one necessary for microtubule assembly by the pericentriolar material. In this regard, it is possible that the small amount of the 37CD γ-tubulin isotype constitutively associated with the centrosomal fraction plays a role in centriole duplication. However, it is unlikely that this low-abundance γ-tubulin isotype plays an important role in the nucleation of mitotic microtubules, as suggested by the absence of microtubules issuing directly from the pericentriolar material. We showed that, after 23C γ-tubulin depletion, the 37CD isotype was not affected; its expression level was maintained and it retained its polar localization. Moreover, under the experimental conditions used, the function of this minor γ-tubulin isotype could not be determined by RNAi, despite the use of two distinct dsRNAs. The poor susceptibility of the 37CD γ-tubulin isoform to the RNAi strategy might stem from its specific properties in *Drosophila* cells, such as its low concentration (Raynaud-Messina et al., 2001), its absence from the cytosolic fraction (Raynaud-Messina et al., 2001) and/or a possible slow turnover.

In 23C γ-tubulin-depleted S2 cells, the centrioles were often shorter than in the control cells. The presence of a short centriole among normal sized centrioles has been noticed in abnormal metaphases of neuroblasts from the *Drosophila Dgrip91* mutants (Barbosa et al., 2000). Centrioles are generally believed to be very stable organelles. However, in *Physarum* amoebae, a transient decrease in the length of the parental centrioles occurs in mitosis, during the assembly of the daughter centrioles (Gely and Wright, 1985). If the γ-tubulin present in the centriole and basal-body lumen (Fuller et al., 1995; Klotz et al., 2003; Moudjou et al., 1996) interacts with the centriolar microtubules, its depletion might well alter centriole morphogenesis, possibly by an action on centriolar microtubule dynamics. Indeed, a role of γ-tubulin in microtubule dynamics and stability has been suggested in *Aspergillus* (Oakley and Oakley, 1989), *Schizosaccharomyces* (Paluh et al., 2000), *Caenorhabditis* (Strome et al., 2001), as well as in mammalian cells, where γ-tubulin interacts with the stable kinetochore microtubules (Lajoie-Mazenc et al., 1994).

γ-Tubulin-depleted *Drosophila* S2 cells mostly assembled half-spindles, resulting in monopolar metaphases with a normal overall microtubule orientation and a 13-protofilament structure. The presence of pericentriolar material was confirmed by electron microscopy and by the recruitment of the centrosomal proteins CP190 and centrosomin, which appeared to be independent of the presence of γ-tubulin (Fig. 4A). Microtubule reassembly after cold treatment suggested that the pole retained a nucleation activity (Fig. 4B). However, consistent with the severe depletion of the main centrosomal γ-tubulin, most of the spindle microtubules were not assembled from the pericentriolar material, which accounted for the absence of astral microtubules. Nucleation resulted at least partially from elongation of the distal extremity of the microtubules of the four centrioles. This process differs from the formation of primary cilia observed in several interphase animal cells (Wheatley, 1982). In mitotic 23C-γ-tubulin-depleted S2 cells, the microtubules produced by the centrioles failed to form the characteristic axonemal structure. They were not surrounded by a membrane and were not associated in microtubule doublets as in typical primary cilia (Wheatley, 1982) but rather diverged in the cytoplasm, giving rise to a few sub-spindles. Moreover, they did not arise from the dispersion of the ensheathing membrane of a primary cilium, as has been reported in cells undergoing early mitosis (Rieder et al., 1979), because primary cilia were not observed in either control or treated interphase cells. It is likely that the distal extremity of the centriolar microtubules was not blocked by regulatory proteins and could assemble α/β-tubulin heterodimers, as observed in vitro with isolated centrioles (Gould and Borisy, 1977). Unless triggered by the specific axonemal program, during normal mitosis, this elongation process remains exceptional (Krishan and Buck, 1965). Our observations suggest that this atypical elongation pathway is normally overridden by the efficiency of nucleation from the high number of γ-tubulin nucleation sites present in the

pericentriolar material. The failure of centriole separation and elongation of the centriolar microtubules we observed is consistent with the formation of monopolar spindles. However, this assembly pathway might only give rise to a limited number of spindle microtubules, unless microtubules detach from the distal ends of the centriole. Alternatively, the presence of additional microtubule bundles on the chromosome face opposite the main pole (Fig. 4G) suggests that microtubules might also be nucleated at the kinetochores. In contrast to the microtubule assembly pathway predominantly mediated by the pericentriolar γ-tubulin (Hannak et al., 2002), our results suggest that, below a critical concentration of γ-tubulin, other assembly mechanisms could contribute to spindle formation. These alternative mechanisms were unable to generate a fully functional mitotic apparatus in most cases.

Taken together, our results demonstrate the inefficiency of the pericentriolar material in promoting microtubule nucleation after depletion of γ-tubulin. They point to an alternative centrosome-driven mechanism of microtubule assembly that might contribute to the formation of abnormal, albeit partially functional, mitotic spindles.

References

Barbosa, V., Yamamoto, R. R., Henderson, D. S. and Glover, D. (2000). Mutation of a *Drosophila* gamma tubulin ring complex subunit encoded by *discs degenerate-4* differentially disrupts centrosomal protein localization. *Genes Dev.* **14**, 3126-3139.

Barette, C., Jariel-Encontre, I., Piechaczyk, M. and Piette, J. (2000). Human cyclin C protein is stabilized by its associated kinase Cdk8, independently of its catalytic activity. *Oncogene* **20**, 551-562.

Basu, J., Bousbaa, H., Logarinho, E., Li, Z. X., Williams, B. C., Lopes, C., Sunkel, C. E. and Goldberg, M. L. (1999). Mutations in the essential spindle checkpoint gene bub1 cause chromosome missegregation and fail to block apoptosis in *Drosophila*. *J. Cell Biol.* **146**, 13-28.

Clemens, J. C., Worby, C. A., Simonson-Leff, N., Muda, M., Maehama, T., Hemmings, B. A. and Dixon, J. E. (2000). Use of double-stranded RNA interference in *Drosophila* cell lines to dissect signal transduction pathways. *Proc. Nat. Acad. Sci. USA* **97**, 6499-6503.

Debec, A., Détraves, C., Montmory, C., Géraud, G. and Wright, M. (1995). Polar organization of gamma-tubulin in acentriolar mitotic spindles of *Drosophila melanogaster* cells. *J. Cell Sci.* **108**, 2645-2653.

De Muth, J. E. (1999). Basic statistics and pharmaceutical statistical applications. New York. Marcel Dekker.

Fava, F., Raynaud Messina, B., Leung Tack, J., Mazzolini, L., Li, M., Guillemot, J. C., Cachot, D., Tollon, Y., Ferrara, P. and Wright, M. (1999). Human 76p: a new member of the gamma-tubulin-associated protein family. *J. Cell Biol.* **147**, 857-868.

Félix, M. A., Antony, C., Wright, M. and Maro, B. (1994). Centrosome assembly in vitro: role of gamma-tubulin recruitment in *Xenopus* sperm aster formation. *J. Cell Biol.* **124**, 19-31.

Fuller, S. D., Gowen, B. E., Reinsch, S., Sawyer, A., Wepf, R. and Karsenti, E. (1995). The core of the mammalian centriole contains gamma-tubulin. *Curr. Biol.* **5**, 1384-1393.

Gely, C. and Wright, M. (1985). Centriole size modifications during the cell cycle of the amoebae of the myxomycete *Physarum polycephalum*. *J. Ultrastruct. Res.* **91**, 127-137.

Gonzales, C., Tavosanis, G. and Mollinari, C. (1998). Centrosomes and microtubule organization during *Drosophila* development. *J. Cell Sci.* **111**, 2697-2706.

Gould, R. R. and Borisy, G. G. (1977). The pericentriolar material in Chinese hamster ovary cells nucleates microtubule formation. *J. Cell Biol.* **73**, 601-615.

Gunawardane, R. N., Martin, O. C., Cao, K., Zhang, L., Dej, K., Iwamatu, A. and Zheng, Y. (2000). Characterization and reconstitution of *Drosophila* γ-tubulin ring complex subunits. *J. Cell Biol.* **151**, 1513-1523.

Hannak, E., Oogema, K., Kirkham, M., Gönczy, P., Habermann, B. and Hyman, A. A. (2002). The kinetically dominant assembly pathway for centrosomal asters in *Caenorhabditis elegans* is gamma-tubulin dependent. *J. Cell Biol.* **157**, 591-602.

Henikoff, S., Ahmad, K., Platero, J. S. and van Steensel, B. (2000). Heterochromatic deposition of centromeric histone H3-like proteins. *Proc. Nat. Acad. Sci.* USA **97**, 716-721.

Jean, C., Tollon, Y., Raynaud-Messina, B. and Wright, M. (1999). The mammalian interphase centrosome: two independent units maintained together by the dynamics of the microtubule cytoskeleton. *Eur. J. Cell Biol.* **78**, 549-560.

Joshi, H. C., Palacios, M. J., McNamara, L. and Cleveland, D. W. (1992). γ-Tubulin is a centrosomal protein required for cell cycle-dependent microtubule nucleation. *Nature* **356**, 80-83.

Julian, M., Tollon, Y., Lajoie-Mazenc, I., Moisand, A., Mazarguil, H., Puget, A. and Wright, M. (1993). Gamma-tubulin participates in the formation of the midbody during cytokinesis in mammalian cells. *J. Cell Sci.* **105**, 145-156.

Klotz, C., Ruiz, F., Garreau-de-Loubresse, N., Wright, M., Dupuis-Williams, P. and Beisson, J. (2003). Gamma-tubulin and MTOCs in *Paramecium*. *Protist* **154**, 193-209.

Krishan, A. and Buck, R. C. (1965). Structure of the mitotic spindle in L-strain fibroblasts. *J. Cell Biol.* **24**, 433-444.

Lajoie-Mazenc, I., Tollon, Y., Détraves, C., Julian, M., Moisand, A., Gueth-Hallonet, C., Debec, A., Salles-Passador, I., Puget, A., Mazarguil, H. et al. (1994). Recruitment of antigenic gamma-tubulin during mitosis in animal cells: presence of gamma-tubulin in the mitotic spindle. *J. Cell Sci.* **107**, 2825-2837.

Leclerc, V., Tassan, J. P., O'Farrell, P. H., Nigg, E. A. and Leopold, P. (1996). *Drosophila* Cdk8, a kinase partner of cyclin C that interacts with the large subunit of RNA polymerase II. *Mol. Biol. Cell* **7**, 505-513.

Leguy, R., Melki, R., Pantaloni, D. and Carlier, M. F. (2000). Monomeric gamma-tubulin nucleates microtubules. *J. Biol. Chem.* **275**, 21975-21980.

Li, K. and Kaufman, T. C. (1996). The homeotic target gene centrosomin encodes an essential centrosomal component. *Cell* **85**, 585-596.

Marschall, L. G., Jeng, R. L., Mulholland, J. and Stearns, T. (1996). Analysis of Tub4p, a yeast gamma-tubulin-like protein: implications for microtubule-organizing center function. *J. Cell Biol.* **134**, 443-454.

Martin, O. C., Gunawardane, R. N., Iwamatsu, A. and Zheng, Y. (1998). Xgrip109: a γ-tubulin-associated protein with an essential role in γ-tubulin ring complex (γ-TuRC) assembly and centrosome function. *J. Cell Biol.* **141**, 675-687.

Megraw, T. L., Li, K., Koa, L.-R. and Kaufman, T. C. (1999). The centrosomin protein is required for centrosome assembly and function during cleavage in *Drosophila*. *Development* **126**, 2829-2839.

Megraw, T. L., Li, K., Koa, L.-R. and Kaufman, T. C. (2001). Zygotic development without functional mitotic centrosomes. *Curr. Biol.* **11**, 116-120.

Moritz, M., Braunfeld, M. B., Sedat, J. W., Alberts, B. and Agard, D. A. (1995a). Microtubule nucleation by γ-tubulin-containing rings in the centrosome. *Nature* **378**, 638-640.

Moritz, M., Braunnfeld, M. B., Fung, J. C., Sedat, J. W., Alberts, B. M. and Agard, D. A. (1995b). Three-dimensional structural characterization of centrosomes from early *Drosophila* embryos. *J. Cell Biol.* **130**, 1149-1159.

Moritz, M., Zheng, Y. X., Alberts, B. M. and Oegema, K. (1998). Recruitment of the gamma-tubulin ring complex to *Drosophila* salt-stripped centrosome scaffolds. *J. Cell Biol.* **142**, 775-786.

Moudjou, M., Bordes, N., Paintrand, M. and Bornens, M. (1996). Gamma-tubulin in mammalian cells: the centrosomal and the cytosolic forms. *J. Cell Sci.* **109**, 875-887.

Murphy, S. M., Preble, A. M., Patel, U. K., O'Connel, K. L., Dias, D. P., Moritz, M., Agard, D., Stults, J. T. and Stearns, T. (2001). GCP5 and GCP6: two new members of the human γ-tubulin complex. *Mol. Biol. Cell* **12**, 3340-3352.

Murphy, S. M., Urbani, L. and Stearns, T. (1998). The mammalian γ-tubulin complex contains homologues of the yeast spindle pole body components Spc97p and Spc98p. *J. Cell Biol.* **141**, 663-674.

Oakley, C. E. and Oakley, B. R. (1989). Identification of γ-tubulin, a new

member of the tubulin superfamily encoded by *mipA* gene of *Aspergillus nidulans*. *Nature* **338**, 662-664.

Oegema, K., Wiese, C., Martin, O. C., Milligan, R. A., Iwamatsu, E., Mitchison, T. J. and Zheng, Y. (1999). Characterization of two related *Drosophila* γ-tubulin complexes that differ in their ability to nucleate microtubules. *J. Cell Biol.* **144**, 721-733.

Paluh, J. L., Nogales, E., Oakley, B. R., McDonald, K., Pidoux, A. L. and Cande, W. Z. (2000). A mutation in gamma-tubulin alters microtubule dynamics and organization and is synthetically lethal with the kinesin-like protein Pkl1p. *Mol. Biol. Cell* **11**, 1225-1239.

Raynaud-Messina, B., Debec, A., Tollon, Y., Garès, M. and Wright, M. (2001). Differential properties of the two *Drosophila* γ-tubulin isotypes. *Eur. J. Cell Biol.* **80**, 643-649.

Rieder, C. L., Jensen, C. G. and Jensen, L. C. W. (1979). The resorption of primary cilia during mitosis in a vertebrate (PtK1) cell line. *J. Ultrastruct. Res.* **68**, 173-185.

Riparbelli, M. G., Callaini, G., Glover, D. M. and Avides, M. D. C. (2002). A requirement for the abnormal spindle protein to organise microtubules of the central spindle for cytokinesis in *Drosophila*. *J. Cell Sci.* **115**, 913-922.

Rotaru, V., Lajoie-Mazenc, I., Tollon, Y., Raynaud-Messina, B., Jean, C., Detraves, C., Julian, M., Moisand, A. and Wright, M. (1999). Condensation-decondensation of the gamma-tubulin containing material in the absence of a structurally visible organelle during the cell cycle of *Physarum plasmodia*. *Biol. Cell* **91**, 393-406.

Rubin, G. M., Yandell, M. D., Wortman, J. R., Miklos, G. L. G., Nelson, C. R., Hariharan, I. K., Fortini, M. E., Li, P. W., Apweiler, R., Fleischmann, W. et al. (2000). Comparative genomics of the eukaryotes. *Science* **287**, 2204-2215.

Ruiz, F., Beisson, J., Rossier, J. and Dupuis-Williams, P. (1999). Basal body duplication in *Paramecium* requires γ-tubulin. *Curr. Biol.* **9**, 43-46.

Sampaio, P., Rebello, E., Varmark, H., Sunkel, C. E. and Gonzalez, C. (2001). Organized microtubule arrays in γ-tubulin-depleted *Drosophila* spermatocytes. *Curr. Biol.* **11**, 1788-1793.

Saunders, R. D. C., Avides, M. C., Howard, T., Gonzalez, C. and Glover, D. M. (1997). The *Drosophila* gene abnormal spindle encodes a novel microtubule-associated protein that associates with the polar regions of the mitotic spindle. *J. Cell Biol.* **137**, 881-890.

Schneider, I. (1972). Cell lines derived from late embryonic stages of *Drosophila melanogaster*. *J. Embrbryol. Exp. Morphol.* **27**, 353-365.

Shu, H. B. and Joshi, H. C. (1995). γ-Tubulin can both nucleate microtubule assembly and self-assemble into novel tubular structures in mammalian cells. *J. Cell Biol.* **130**, 1137-1147.

Shu, H. B., Li, Z., Palacios, M. J., Li, Q. and Joshi, H. C. (1995). A transient association of gamma-tubulin at the midbody is required for the completion of cytokinesis during the mammalian cell division. *J. Cell Sci.* **108**, 2955-2962.

Spang, A., Geissler, S., Grein, K. and Schiebel, E. (1996). Gamma-tubulin-like Tub4p of *Saccharomyces cerevisiae* is associated with the spindle pole body substructures that organize microtubules and is required for mitotic spindle formation. *J. Cell Biol.* **134**, 429-441.

Stearns, T. and Kirschner, M. (1994). In vitro reconstitution of centrosome assembly and function: the central role of γ-tubulin. *Cell* **76**, 623-637.

Strome, S., Powers, J., Dunn, M., Reese, K., Malone, C. J., White, J., Seydoux, G. and Saxton, W. (2001). Spindle dynamics and the role of gamma-tubulin in early *Caenorhabditis elegans* embryos. *Mol. Biol. Cell* **12**, 1751-1764.

Sunkel, C. E., Gomes, R., Sampaio, P., Perdigao, J. and Gonzalez, C. (1995). Gamma-tubulin is required for the structure and function of the microtubule organizing centre in *Drosophila* neuroblasts. *EMBO J.* **14**, 28-36.

Tassin, A. M., Celati, C., Moudjou, M. and Bornens, M. (1998). Characterization of the human homolog of the yeast Spc98p and its association with γ-tubulin. *J. Cell Biol.* **141**, 689-701.

Tavosanis, G., Llamazares, S., Goulielmos, G. and Gonzalez, C. (1997). Essential role for γ-tubulin in the acentriolar female meiotic spindle of *Drosophila*. *EMBO J.* **16**, 1809-1819.

Tilney, L. G., Bryan, J., Bush, D. J., Fujiwara, K., Mooseker, M. S., Murphy, D. G. and Snyder, D. H. (1973). Microtubules: evidence for 13 protofilaments. *J. Cell Biol.* **59**, 267-275.

Wakefield, J. G., Bonaccorsi, S. and Gatti, M. (2001). The *Drosophila* protein Asp is involved in microtubule organization during spindle formation and cytokinesis. *J. Cell Biol.* **153**, 637-647.

Wheatley, D. N. (1982). *The Centriole: A Central Enigma of Cell Biology*. Amsterdam, The Netherlands: Elsevier Biomedical Press, North-Holland.

Whitfield, W. G. F., Millar, S. E., Saumweber, H., Frasch, M. and Glover, D. M. (1988). Cloning of a gene encoding an antigen associated with centrosome in *Drosophila*. *J. Cell Sci.* **89**, 467-480.

Wiese, C. and Zheng, Y. (2000). A new function for the γ-tubulin ring complex as a microtubule minus-end cap. *Nature* **2**, 358-364.

Wittmann, T., Hyman, A. and Desai, A. (2001). The spindle: a dynamic assembly of microtubules and motors. *Nat. Cell Biol.* **3**, E28-E34.

Zhang, L., Keating, T. J., Wilde, A., Borisy, G. G. and Zheng, Y. (2000). The role of Xgrip210 in γ-tubulin ring complex assembly and centrosome recruitment. *J. Cell Biol.* **151**, 1525-1535.

Zheng, Y., Wong, M. L., Alberts, B. and Mitchison, T. (1995). Nucleation of microtubule assembly by a γ-tubulin-containing ring complex. *Nature* **378**, 578-583.